Novel Polymeric Metal Complexes for Dye Sensitizer : Synthesis and Photovoltaic Performances

Houpeng Zhang
Xiangtan University https://orcid.org/0000-0003-4646-1163
xianming wu
Xiangtan University
yong tian
Xiangtan University
kaixuan wang
Xiangtan University
shiyu tang
Xiangtan University
chaofan zhong (zhongcf798@xtu.edu.cn)
Xiangtan University https://orcid.org/0000-0002-2422-2711

Research Article

Keywords: polymeric metal complex, the coordination metals (Cd, Zn, Cu, Ni), auxiliary electron acceptor, dye-sensitized solar cells.

Posted Date: November 9th, 2021

DOI: https://doi.org/10.21203/rs.3.rs-1049502/v1

Version of Record: A version of this preprint was published at Journal of Inorganic and Organometallic Polymers and Materials on January 17th, 2022. See the published version at https://doi.org/10.1007/s10904-021-02220-w.

Abstract

Four novel polymeric metal complexes with a D-A-π-A motif, BDTT-PY-Cd, BDTT-PY-Zn, BDTT-PY-Cu and BDTT-PY-Ni, were designed, synthesized and characterized. These polymeric metal complexes were made up with Cd(Ⅱ), Zn(Ⅱ), Cu(Ⅱ), Ni(Ⅱ) complexes, thienylbenzo-[1,2-b:4,5-b'] dithiophene (BDTT) and the 8-quinolinol derivative, which were used severally as dye sensitzers' auxiliary electron acceptors (A), electron donor (D) and π bridges as well as the acceptors (A). Under AM 1.5 irradiation (100 mW cm^{-2}), the devices of dye sensitized solar cells (DSSC) based on four polymer complexes exhibited short-circuit photocurrent densities (J_{sc}) of 17.45 mA cm^{-2}, 14.75 mA cm^{-2}, 13.94 mA cm^{-2}, and 12.00 mA cm^{-2}, as well as attractive power conversion efficiencies (PCE) of were 9.73 %, 8.02 %, 6.82 % and 6.12 %, respectively. The photovoltaic conversion efficiency (PCE) and short-circuit photocurrent density (J_{sc}) of BDTT-PY-Cd, BDTT-PY-Zn, BDTT-PY-Cu and BDTT-PY-Ni decrease in order because the radius and charge number of the metal ion affect the strength of the coordination bond between the metal ion and the ligand. These results provides a new way of development for efficient and stable dye sensitizers in the future.

1. Introduction

Dye-sensitised solar cells (DSSCs) are a kind of organic solar cell proposed by Gratzel and O'regan in 1991 [1], have received continuous attention from a large number of researchers in recent years due to their simple and inexpensive manufacturing process, light weight and continuous breakthroughs in photoelectric conversion efficiency [2-3]. The photovoltaic performance of DSSCs is basically controlled by multi-channel charge transfer kinetics, charge regeneration and light absorption, which mainly depends on the dye sensitizer [4].

To date, dye sensitizers have mainly been divided into the following two categories: 1) Metal organic dyes: Ruthenium (Ru(II)) complexes are considered to be the most successful and representative dye sensitizers for DSSCs due to its wide-range solar absorption spectra and good photovoltaic performance [5-7]. However, it has the following disadvantages: i) limited absorption in the NIR region of the spectrum; ii) complexed purification steps; iii) limited resources of precious metals [8-9]. 2) Metal-free organic dyes: donor-π-bridge-acceptor (D-π-A) structures are common for organic dyes and show higher efficiency, better push-pull balance and enhanced light absorption in p-type DSSCs compared to Ru(II) complexes [9,10-11]. However, this structure also has its own drawbacks, such as low thermal stability, narrow absorption range, and charge recombination [12,13]. Because of these shortcomings, the advent of the D-A-π-A motif of dye sensitizers has led to a new generation of better performing metal-free organic dyes [14].

In the D-A-π-A motif of dye sensitizers, an organic electron-withdrawing conjugated group such as benzothiadiazole (BTD) [15], benzotriazole (BTZ) [16], quinoxaline (Qu) [17], phthalimide [18] and diketo-pyrrolopyrrole (DPP) [19] has been introduced into the π-bridge on the basis of D-π-A framework to act as auxiliary electron acceptor (A), which can reduce effectively electron recombination and promote the transfer of electrons in molecule. In addition, auxiliary electron acceptor not only can the push-pull

electron balance and open-circuit voltage inside the molecule be improved, but also the photovoltaic performance can be greatly improved [20,21]. Many researchers studied systematically the auxiliary electron acceptor which can increased the efficiency of D-A-π-A motif sensitizers from about 5% to more than 10% and improved greatly the thermal stability of the devices [22-25]. In contrast to organic auxiliary electron acceptor, the electron-withdrawing ability of the auxiliary electron acceptor employing metal complexes as electron-withdrawing group can be enhanced by modulating the orbital energy level, strengthening charge separation, and increasing the open circuit voltage, which can achieve significant improvement in stability and photoelectric conversion efficiency. [26-28].

To study how the auxiliary electron acceptor (A) of metal complexes effect the photovoltaic performance of the dye sensitizers, a series of polymeric metal complexes dye sensitizers with metal complexes of pyrrole derivatives as auxiliary electron acceptors were designed and synthesized. What's more, systematical study of the influence about metal complexes' coordination bonds in different strength on the photovoltaic performance was investigated.

2. Experimental Section

2.1 Materials.

All chemical reagents were obtained from Shanghai Macklin Biochemical Technology Co. Ltd (Shanghai, China) and were used without further purification, except that BDTT was procured from Shanghai aladdin Biochemical Technology Co. Ltd (Shanghai, China). Other reagents and solvents were purchased commercially as analytical-grade quality and used without further purification.

2.2 Instruments and Measurements.

^{1}H NMR and ^{13}C NMR spectra were recorded on an ARX400 NMR spectrometer from Bruker using $CDCl_3$ or DMSO-d_6 as solvent and tetramethylsilane (TMS, δ = 0.00 ppm) as internal standard. Fourier transform infrared spectroscopy testing (FT-IR) was performed using a Nicolet Model 6700 infrared spectrometer from Nicholl, U.S.A. Sample preparation was performed using the KBr press method. The samples were mixed with dry KBr in the ratio of 1:100 and then pressed, and the wave number scanning range was 4000~400 cm^{-1}. Elemental analysis were performed using a Vario El III elemental analyzer from Elemental Analysis Systems, Germany, which was burned in an oxygen-filled environment for measuring the C, H, and N content of the samples. Thermogravimetric analysis (TGA) was performed using SDT Q50 thermal weight loss analyzer produced by TA, USA, to test the thermal decomposition temperature (T_d) of the samples under Nitrogen atmosphere, with a temperature range of 25~800 ℃ and a ramping rate of 20 ℃/min. The cyclic voltammetry (CV) test was performed in a three-electrode system using a CHI650D electrochemical workstation, with the working electrode, the comparison electrode and the reference electrode using a glassy carbon electrode, a platinum electrode and a saturated mercury electrode (SCE), respectively, with a scanning speed of 100 mV/s. The electrolyte was a ferrocene internal standard containing a concentration of 3×10^{-5} mol/L and a concentration of 0.1 mol/L of tetrabutylammonium

tetrafluoroborate (SCE). Butylammonium tetrafluoroborate ($(n\text{-}C_4H_9)_4N^+BF_4^-$) in acetonitrile solution, and the sample was prepared as a solution and then added dropwise to the working electrode to make a membrane. The gel permeation chromatography (GPC) test was performed using a Waters-1515 medium temperature gel permeation chromatograph with THF as the mobile phase at a flow rate of 1.0 mL/min, a column temperature of 80°C and polystyrene solution as the reference. The ultraviolet-visible absorption spectroscopy test (UV-Vis) was performed using a Cary 100 UV-Vis spectrometer from Agilent, USA, and the sample was prepared as a DMF solution with a concentration of 1×10-5 mol/L and tested at room temperature.Differential scanning calorimetric analysis (DSC) was performed using a Q10 thermal analysis tester from PA, USA, with a heating rate of 20 ℃/min and a temperature range of 25-250 ℃ under nitrogen atmosphere.

2.3 Fabrication of DSSCs [29-30].

TiO_2 slurry with particle size of 20 nm and aperture of 24 nm was poured into the wire mesh plate by screen printing method, and printed on the conductive substrate to form a film with thickness of 9~10 μm, and dried at 125 ℃ for 6 minutes. After deposition, the conductive substrate should be dried at 125 ℃ for about 5 minutes. Then, the prepared TiO_2 films were placed in a capillary furnace and calcined by programmed heating, baking at 325°C for 5 min, 375°C for 5 min, 450°C for 15 min, and 500°C for 15 min, respectively. After calcining, $TiCl_4$ (0.04 mol/L) solution was further treated at 70 ℃ for 0.5 h, then washed with water and anhydrous ethanol, then put into muffle furnace again, and calcined at 500 ℃ for 30 min to prepare the titanium dioxide photoanode. The TiO_2 film was soaked in 2×10^{-4} mol/L dyes (for BDTT-PY-Cd, BDTT-PY-Zn, BDTT-PY-Cu, and BDTT-PY-Ni) in DMF solution and stirred for 24 hours at room temperature. After calcining the photoanode, the temperature drops to 40 ℃, the dye was immersed in the above solution and treated in the dark for 36 hours, then washed with DMF and ethanol successively, and finally vacuum dried. The solution of H_2PtCl_6 (0.02mol /L, isopropanol as solvent) was coated on the conductive substrate (FTO) with holes, and calcined at 400 ℃ for 15 min to prepare the electrodes. Acetonitrile was used as the solvent to prepare an electrolyte, in which the iodine (0.05 mol/L), lithium iodide (0.1 mol/L), 4-tert-butyl pyridine (0.5 mol/L), and 1, 2-dimethyl-3-propyl imidazolidine (0.6 mol/L).

2.4 Synthesis.

The routes of four polymeric metal complexes BDTT-PY-Cd, BDTT-PY-Zn, BDTT-PY-Cu and BDTT-PY-Ni are shown in Scheme 1, and the detailed synthesis steps of the four polymeric metal complexes can be queried in the supporting information.

3. Result And Discussion

3.1 Synthesis and Characterization of Polymeric Metal Complexes.

It can be seen from Scheme 1, -Pyridin-3-yl-1H-pyrrole-2-carbaldehyde (**1**) was attained by Ma Dawei carbon nitrogen coupling reaction of 3-Bromo-pyridine and pyrrole-3-carboxaldehyde, 3-(2-Vinyl-pyrrol-1-yl)-pyridine (**2**) was prepared from 1-Pyridin-3-yl-1H-pyrrole-2-carbaldehyde by addition reaction of aldehyde group, 5-Vinyl-quinolin-8-ol (**3**) was synthesized by Reimer-Tiemann reaction of 8-hydroxyqzlinoline. The synthesis of 2-cyano-3-(8-hydroxy-quinolin-5-yl)acrylic acid (**4**) was gained by 8-hydroxyqzlinoline and cyanoacetic acid. The NMR spectra of compound **1**, **2**, **3** and **4**, are shown in **Fig. S1**, **Fig. S2**, **Fig. S3** and **Fig. S4**, respectively. The four target polymeric metal complexes were obtained by Yamamoto coupling reaction of metal complexes PY-Cd, PY-Zn, PY-Cu and PY-Ni with BDTT.

Table 1 summarizes the results of elemental analysis, FT-IR spectroscopy and gel permeation chromatography (GPC) for the four polymer metal complexes.The data of GPC show that the number average molecular weights (Mn) of BDTT-PY-Cd, BDTT-PY-Zn, BDTT-PY-Cu and BDTT-PY-Ni are 11.79, 10.11, 12.62 and 10.05 kg mol^{-1}, with PDI values ranging from 1.84 to 2.11 and N values of 8, 9, 10 and 8 for the four dyes, respectively.These results, together with the elemental analysis, reflect that the four target polymers have been successfully synthesized.

The FT-IR spectra of metal complexes (PY-Cd, PY-Zn, PY-Cu and PY-Ni) and the four polymeric metal complexes (BDTT-PY-Cd, BDTT-PY-Zn, BDTT-PY-Cu and BDTT-PY-Ni) are shown in **Fig. S5** and **Fig. S6**.

According to **Fig. S5**, the peak around 3420 cm^{-1} is the hydroxyl peak, which is the stretching vibration peak of the hydroxyl group; The absorption peak around 2210 cm^{-1} is the C≡N absorption peak on the auxiliary ligand. The absorption peak for C=C is around 1610 cm^{-1} and the absorption peak for C=N is around 1565 cm^{-1}. The absorption peaks for the four metal complexes C-O-M occur at around 1110 cm^{-1} and N-M at around 505 cm^{-1}. Notably, the absorption peak of PY-Cu at 1686 cm^{-1} is generated by the stretching vibration of C=O. However, the other complexes do not have significant absorption peaks in the vicinity, which is due to the strong absorption peaks in the vicinity covering the stretching vibration peaks of C=O.

As seen in **Fig. S6**, the C-O-M absorption peaks of BDTT-PY-M appear at 1103 cm^{-1}-1112 cm^{-1} and N-M absorption peaks appear at 493 cm^{-1}-515 cm^{-1}. Compared with the corresponding complexes, the absorption peaks of the above functional groups are having a certain redshifted, which attributed to expanding the conjugate system by introducing the BDTT. At about 2920 cm^{-1} and 2850 cm^{-1}, the C-H stretching vibration peak of the alkyl chain appeared, which further indicated that the donor BDTT had been successfully introduced into the polymer. Combined with the results of gel permeation chromatography and elemental analysis, the four polymeric metal complexes have been synthesized successfully.

3.2 Photophysical Properties of Polymeric Metal Complexes.

According to the UV-Vis spectrum of PY-M and BDTT-PY-M (Fig. 1), the maximum absorption wavelengths of PY-Cd, PY-Zn, PY-Cu and PY-Ni occur at 373 nm, 362 nm, 348 nm and 342 nm respectively, this may be due to the stronger electronic interactions between the larger radius coordination metals and the same

ligands. The corresponding polymeric metal complexes (BDTT-PY-Cd, BDTT-PY-Zn, BDTT-PY-Cu and BDTT-PY-Ni) have two absorption peaks. The polymer metal complexes have a certain red shift in the 350-400 nm range compared to the corresponding complexes. This is may be due to BDTT of strong electronic capability and good planarity was introduced. Notably, the polymeric metal complexes have an extra absorption peak with a maximum absorption wavelength of 506 nm, 488 nm, 478 nm and 464 nm respectively, which is due to the charge transfer between the

Table 1
Molecular weights and thermal properties of four polymeric metal complexes BDTT-PY-Cd, BDTT-PY-Zn, BDTT-PY-Cu and BDTT-PY-Ni

polymer	M_n[a][×10^3g mol^{-1}]	M_w[a][×10^3g mol^{-1}]	*PDI*	N	T_g[b][°C]	T_d[c][°C]
BDTT-PY-Cd	11.79	22.75	1.93	8	163	314
BDTT-PY-Zn	10.11	20.62	2.04	9	154	296
BDTT-PY-Cu	12.62	26.62	2.11	10	149	287
BDTT-PY-Ni	10.05	18.49	1.84	8	142	268
[a] *Determined by gel permeation chromatography with polystyrene as standard.*						
[b] *Determined by DSC with a heating rate of 20 °C/min under nitrogen.*						
[c] *The temperature at 5% weight loss under nitrogen.*						

donor BDTT and the complex in the molecule. By comparing the absorption spectra between different polymeric metal complexes, it was found that the maximum absorption wavelength of the polymeric with large coordination metal radius has a certain degree of red shift relative to the polymeric with small coordination metal radius. This may be due to the stronger the feedback π bond formed by the coordination metal with a large radius and the better plane configuration.

According to Table 1, the absorption coefficients of the four polymeric metal complexes were all above 18000 $L{\cdot}mol^{-1}cm^{-1}$ for the maximum absorption wavelength. Among them, BDTT-PY-Cd has the largest absorption of 23,357 L-mol-1cm-1, which reflects the high absorption coefficient of the polymeric metal complexes. In summary, the molecular design of polymeric metal complexes can broaden the spectral absorption range of this class of dyes by introducing ligand metals with strong coordination ability.

3.3 Electrochemical Properties of Polymeric Metal Complexes.

The highest occupied molecular orbital (HOMO) and lowest unoccupied molecular orbital (LUMO) energy levels of the dye sensitiser can estimate the cyclic voltammogram (CV) for the onset of oxidation (E_{ox}) and reduction potential (E_{red}). A suitable energy level can be effective in improving the efficiency of the dye. The HOMO and LUMO energy levels and the electrochemical band gap (E_g) of the polymeric metal complexes can be calculated according to reference [37].

The cyclic voltammetry curves of the four polymers and ferrocene, Fig. 2 shows the HOMO and LUMO energy levels of BDTT-PY-Cd, BDTT-PY-Zn, BDTT-PY-Cu and BDTT-PY-Ni and the data is collected in Table 2. The E_{ox} of four polymers are 0.996, 1.011, 1.034 and 1.135 V, respectively; and their HOMO are respectively -5.336, -5.351, -5.374 and -5.475 eV, which was significantly lower than the redox potential (-4.83 eV) [38] of I^-/I_3^-, indicating that the polymeric metal complexes could be effectively regenerated. The E_{red} of four polymers are -1.049, -1.055, -1.071 and -1.026 V respectively; and their LUMO energy levels are -3.291, -3.285, -3.269 and -3.314 eV respectively, which are higher than the titanium dioxide conduction band energy levels (-4.26 eV) by about 0.97eV, indicating that there is sufficient driving force to make electron injection into the semiconductor. The electrochemical band gaps (E_g) of BDTT-PY-Cd, BDTT-PY-Zn, BDTT-PY-Cu and BDTT-PY-Ni were 2.045, 2.066, 2.105 and 2.161 eV respectively, have smaller energy level gaps and can achieve light absorption in a longer wavelength range. The energy level gap of BDTT-PY-Cd is the smallest, which can explain why the absorption range of UV-Vis absorption spectrum is the largest.

Table 2
Optical and electrochemical property of four polymeric metal complexes BDTT-PY-Cd, BDTT-PY-Zn, BDTT-PY-Cu and BDTT-PY-Ni.

Polymer	$\lambda_{a,max}$ (nm)	ε_{max} (L $mol^{-1}cm^{-1}$)	E_{red} (V)	E_{ox} (V)	HOMO (eV)	LUMO (eV)	E_g (eV)
BDTT-PY-Cd	506	23357	-1.049	0.996	-5.336	-3.291	2.045
BDTT-PY-Zn	488	22072	-1.055	1.011	-5.351	-3.285	2.066
BDTT-PY-Cu	478	20069	-1.071	1.034	-5.374	-3.269	2.105
BDTT-PY-Ni	464	18541	-1.026	1.135	-5.475	-3.314	2.161

3.4 Thermal Propertiesof Polymeric Metal Complexes.

The actual working conditions of dye sensitisers are generally at high temperatures, so good thermal stability of the sensitiser is required for practical use. The thermal properties of the four polymeric metal complexes were measured using thermogravimetric analysis (TGA) and differential scanning calorimetry (DSC) at a

heating rate of 20°C/min under a nitrogen atmosphere. The four polymeric metal complexes (BDTT-PY-Cd, BDTT-PY-Zn, BDTT-PY -Cu and BDTT-PY-Ni) show outstanding thermal stability, as shown in Fig. 3, with data collected in Table 1, and their onset decomposition temperatures (T_d) of 314, 296, 287 and 268°C, respectively. In contrast, their glass transition temperatures (T_g) were 163, 154, 149 and 142°C, respectively. In addition, since no fixed melting point was detected, it was speculated that the four polymers were amorphous structures. These data show that these four polymers are good enough for DSSC applications and that they have excellent thermal stability.

3.5 Photovoltaic Properties of Polymeric Metal Complexes.

The photovoltaic performance tests in DSSCs are mainly used to evaluate the potential of dye sensitisers for application into DSSCs. Photovoltaic devices in DSSCs consisting of polymers were fabricated according to standard procedures and their performance parameters were obtained by testing at standard light intensities (AM 1.5G, 100 mW/cm^2). Fig. 4 shows the photocurrent-photovoltage (*J-V*) curves for the polymeric metal complexes (BDTT-PY-Cd, BDTT-PY-Zn, BDTT-PY-Cu and BDTT-PY-Ni). The test data related to open circuit voltage (V_{oc}), short circuit current density (J_{sc}), fill factor (*ff*) and incident photon-to-current conversion efficiency (IPCE) are shown in Table 3 and Fig. 5.

According to Fig. 4, the short-circuit current densities (J_{sc}) of the four polymeric metal complexes were BDTT-PY-Cd (17.45 mA/cm^2), BDTT-PY-Zn (14.75 mA/cm^2), BDTT-PY-Cu (13.94 mA/cm^2) and BDTT-PY-Ni (12.00 mA/cm^2), respectively. This is consistent with the UV-vis absorption test results, indicating that the better the

absorption spectrum, the higher the photocurrent generated. The open-circuit voltage (V_{oc}) of the four polymeric metal complexes were 0.78, 0.76, 0.74 and 0.75 V, respectively, with corresponding fill factors (ff) of 70.38, 70.43, 71.70, and 66.91%, respectively. The above experimental data indicated that J_{sc} is the most important factor affecting the efficiency of the polymeric. The BDTT-PY-Cd has the highest

PCE with 9.73 %, which is to be attribute to a larger radius, better planarity, and stronger intramolecular electron transfer ability of the polymeric. As shown in Fig. 5, the IPCE curve of the four polymeric metal complexes is over 65 %, among which BDTT-PY-Zn and BDTT-PY-Cd exceed 70 %. The IPCE curve is basically consistent with the UV-visible absorption curve, which further reflects the photoelectric performance of the polymeric metal complex.

Table 3
Photovoltaic parameters of devices based on four polymeric metal complexes BDTT-PY-Cd, BDTT-PY-Zn, BDTT-PY-Cu and BDTT-PY-Ni in DSSCs at full sunlight (AM 1.5 G, 100 mW cm^{-2})

Polymer	Solvent	J_{sc}(mA cm^{-2})	V_{oc}(V)	*ff*(%)	η (%)
BDTT-PY-Cd	DMF	17.45	0.78	70.38	9.73
BDTT-PY-Zn	DMF	14.75	0.76	70.43	8.02
BDTT-PY-Cu	DMF	13.94	0.74	71.70	6.82
BDTT-PY-Ni	DMF	12.00	0.75	66.91	6.12

4. Conclusion

In conclusion, four novel polymeric metal complexes (BDTT-PY-Cd, BDTT-PY-Zn, BDTT-PY-Cu and BDTT-PY-Ni) were successfully synthesized and characterized using metal complexes of pyrrole derivatives with Cd(II), Zn(II), Cu(II) and Ni(II) as auxiliary electron acceptors (A), which can be used as dye sensitizers. According to the photovoltaic test results of the four polymeric metal complexes, the power conversion efficiency (PCE) of BDTT-PY-Cd (9.73%) was higher than that of BDTT-PY-Zn (8.02%), BDTT-PY-Cu (6.82%) and BDTT-PY-Ni (6.12%), and the short-circuit current density (J_{sc}) showed that, in order, BDTT-PY-Cd (17.45 mA cm^{-2}) > BDTT-PY-Zn (14.75 mA cm^{-2}) > BDTT-PY-Cu (13.94 mA cm^{-2}) > BDTT-PY-Ni (12.00 mA cm^{-2}), which is mainly influenced by the metal ions, since the radius and charge number affect the ligand bond strength of the metal ions to the ligand. At the same charge number, larger radius of the metal ion led to stronger coordination bond. In another word, auxiliary acceptor of metal complexes' electron-withdrawing ability and electron-transfer ability between donor (BDTT) and the electron acceptor were enhanced, which can decrease the E_g of polymeric metal complexes and cause red-shift of absorption spectrum λ_{max} of polymeric metal complexes, and increase the short-circuit current densities (J_{sc}) and power conversion efficiency (PCE). This research work provides a new idea for the development of the dye sensitizer with high photovoltaic properties.

Declarations

Acknowledgements

We appreciate the financial support of the Open Project Program of Key Laboratory of Environmentally Friendly Chemistry and Applications of Ministry of Education, China (Grant No. 19HJYH10).

References

1. O'Regan. B, Grätzel. M, Nature. **353**, 737–740 (1991)

2. X. Y. Zhang, Y. Y. Xu, F. Giordano, M. Schreier, N. Pellet, Y. Hu, C. Y. Yi, N. Robertson, J. L. Hua, S. M. Zakeeruddin, H. Tian, M. Grätzel, J. Am. Chem. Soc. **138**, 10742–10745. (2016)
3. I. Chung, B. H. Lee, J. Q. He, R. P. H. Chang, M. G. Kanatzidis, Nature. **485**, 486–489 (2012)
4. N. Kaneza, J.T. Zhang, H.Y. Liu, P. S. Archana, Z. C. Shan, M. Vasiliu, S. H. Polansky, D. A. Dixon, R. E. Adams, R. H. Schmehl, A. Gupta, S. L. Pan, J. Phys. Chem. C. **120**, 9068–9080 (2016)
5. A. B. Athanas, K. Subramaniam, S. Thangaraj, S. Kalaiyar, Int. J. Energy. Res. **44**, 1899–1908 (2020)
6. I. Purnama, S. Salmahaminati, M. Abe, M. Hada,Y. Kubo, J. Y. Mulyana, Dalton. Trans. **48**, 688–695 (2019)
7. Salmahaminati, M. Abe, I. Purnama, J. Y. Mulyana, M. Hada, ACS. Omega. **6**, 55–64 (2021)
8. P. Wang, B. Wenger, R. Humphry-Baker, J. E. Moser, J. Teuscher, W. Kantlehner, J. Mezger, E. V. Stoyanov, S. M. Zakeeruddin, M. Grätzel, J. Am. Chem. Soc. **127**, 6850–6856 (2005)
9. Y. Z. Wu, W. H. Zhu, S. M. Zakeeruddin, M. Grätzel, ACS Appl. Mater. Interfaces. **7**, 9307–9318 (2015)
10. A. Hagfeldt, G. Boschloo, L.C. Sun, L. Kloo, H. Pettersson, Chem. Rev. **110**, 6595–6663 (2010)
11. A. Mishra, K. R. Markus, D. C. Fischer, P. Bäuerle, Angew. Chem. Int. Ed. **48**, 2474–2499 (2009)
12. R. K. Chen, X. C. Yang, H. N. Tian, X. N. Wang, A. Hagfeldt, L. C. Sun, Chem. Mater. **19**, 4007–4015 (2007)
13. M. Liang, J. Chen, Chem. Soc. Rev. **42**, 3453–3488 (2013)
14. Y. Z. Wu, X. Zhang, W. Q. Li, Z. S. Wang, H. Tian, W. H. Zhu, Adv. Energy. Mater. **2**, 149–156 (2012)
15. H. B. Zhu, W. Q. Li,Y. Z. Wu, B. Liu, S. Q. Zhu, X. Li, H. Ågren, W. H. Zhu, ACS. Sustainable. Chem. Eng. **2**, 1026–1034 (2014)
16. Y. Cui, Y. Z. Wu, X. F. Lu,X. Zhang,G. Zhou, F. B. Miapeh, W. H. Zhu, Z. S. Wang, Chemistry of Materials. **23**, 4394–4401 (2011)
17. K. Pei,Y. Z. Wu, H. Li,Z. Y. Geng, H. Tian, W. H. Zhu, ACS. Appl. Mater. Interfaces. **7**, 5296–5304 (2015)
18. W. Q. Li,Y. Z. Wu, Q. Zhang, H. Tian, W. H. Zhu, ACS Appl. Mater. Interfaces. **4**,1822–1830 (2012)
19. S. Y. Qu, C. J. Qin, A. Islam,Y. Z. Wu,W. H. Zhu, J. L. Hua, H. Tian, L. Y. Han, Chem. Commun. **48**, 6972–6974 (2012)
20. Y. Z. Wu, W. H. Zhu, Chem. Soc. Rev. **42**, 2039–2058 (2013)
21. Y. Z. Wu, W. H. Zhu, S. M. Zakeeruddin, M. Grätzel, ACS. Appl. Mater. Interfaces. **18**, 9307–9318 (2015)
22. J. Yuan, Y. Q. Zhang, L. Y. Zhou,G. C. Zhang, H. L. Yip,T. K. Lau, X. H. Lu, C. Zhu, H. j. Peng, P. A. Johnson, M. Leclerc,Y. Cao, J. Ulanski,Y. F. Li,Y. P. Zou, Joule. **3**,1140–1151 (2019)
23. Y. Cui, H. Yao, J. Q. Zhang, K. H. Xian, T. Zhang, L. Hong, Y. M. Wang, Y. Xu, K. Q. Ma, C. B. An, C. He, Z.X. Wei, F. Gao, J. H. Hou, Adv Mater. **32**, 1908205 (2020)
24. P. P. Heng, B. B. An, H. H. Ren, Y. H. Hu, X. G. Guo, L. M. Mao, L. Wang, J. L. Zhang, J. Phys. Chem. C. **124**, 15036–15044 (2020)
25. Z. D. Sun, M. F. He, K. Chaitanya, X. H. Ju, Materials Chemistry and Physics. **248**, 122943 (2020)

26. J. S. Ni, K. C. Ho, K. F. Lin, J. Mater. Chem A. **1**, 3463–3470 (2013)
27. H. P. Zhang, X. M. Wu, S. S. Tang, K. X. Wang, Y. Tian, C. F. Zhong, Appl. Organomet. Chem. e6220 (2021)
28. X. G. Yu, G. J. Wen, J.Y. Deng, X. L. Jin , J. Zhou, W. Zhang, C. F. Zhong, J. Inorg. Organomet. Polym. **23**, 579–586 (2013).
29. H. T. Chan, C. S. K. Mak, A. B. Djurišić, W. K. Chan, Macromolecular Chemistry and Physics. **212**, 774–784 (2011)
30. Z. X. Pan, G. Leem, S. Cekli, K. S. Schanze, ACS Applied Materials & Interfaces. **7**, 16601–16608 (2015)
31. H. Zhang, Q. Cai, D. W. Ma, The Journal of organic chemistry. **70**, 5164-5173 (2005)
32. J. F. Morin, N. Drolet, Y. Tao, M. Leclerc, Chemistry of Materials. **16**, 4619–4626 (2004)
33. Y. T. Chen, H. L. Wang, L. Wan,Y. Z. Bian, J. Z. Jiang, Journal of Organic Chemistry. **76**, 3774–3781 (2011)
34. J. A. Mikroyannidis, Polymer. **36**, 1287–1293(1995)
35. S. A. Abdel-Latif, H. B. Hassib,Y. M. Issa, Spectrochimica. Acta. Part. A Molecular & Biomolecular. Spectroscopy. **67**, 950–957(2007)
36. Z. N. Bao, Y. M. Chen, L. P. Yu, Macromolecules. **27**, 4629–4631(1994)
37. I. Chung, B. Lee, J. Q. He, R. P. H. Chang, M. G. Kanatzidis, Nature. **485**, 486–489 (2012)
38. K. Srinivas, C. R. Kumar, M. A. Reddy, K. Bhanuprakash, V. Ja. Rao, L. Giribabu, Synthetic. Metals. **161**, 96–105 (2011)

Figures

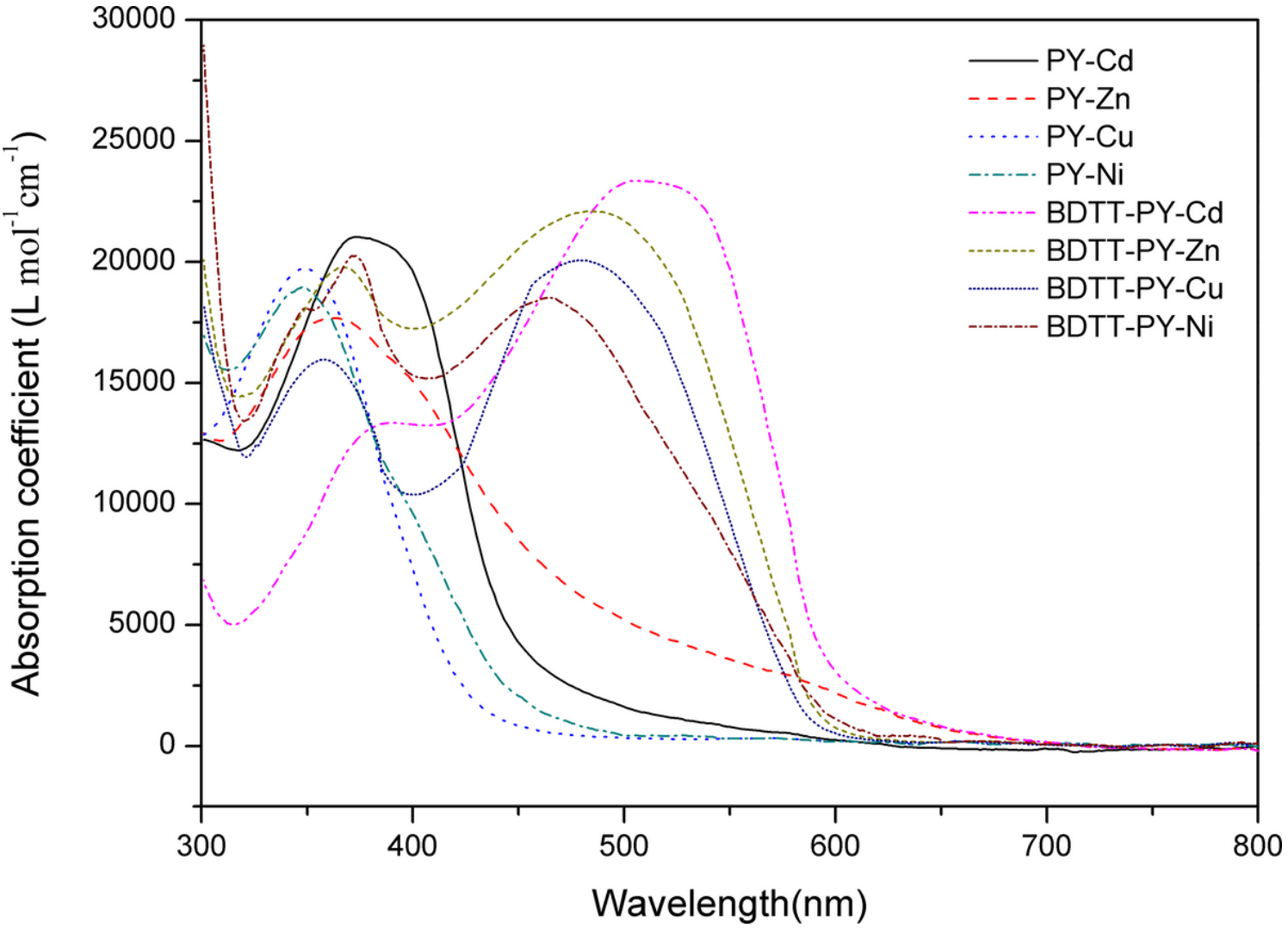

Figure 1

UV–Vis absorption spectra of four metal complexes PY-Cd, PY-Zn, PY-Cu, PY-Ni and four polymeric metal complexes BDTT-PY-Cd, BDTT-PY-Zn, BDTT-PY-Cu, BDTT-PY-Ni.

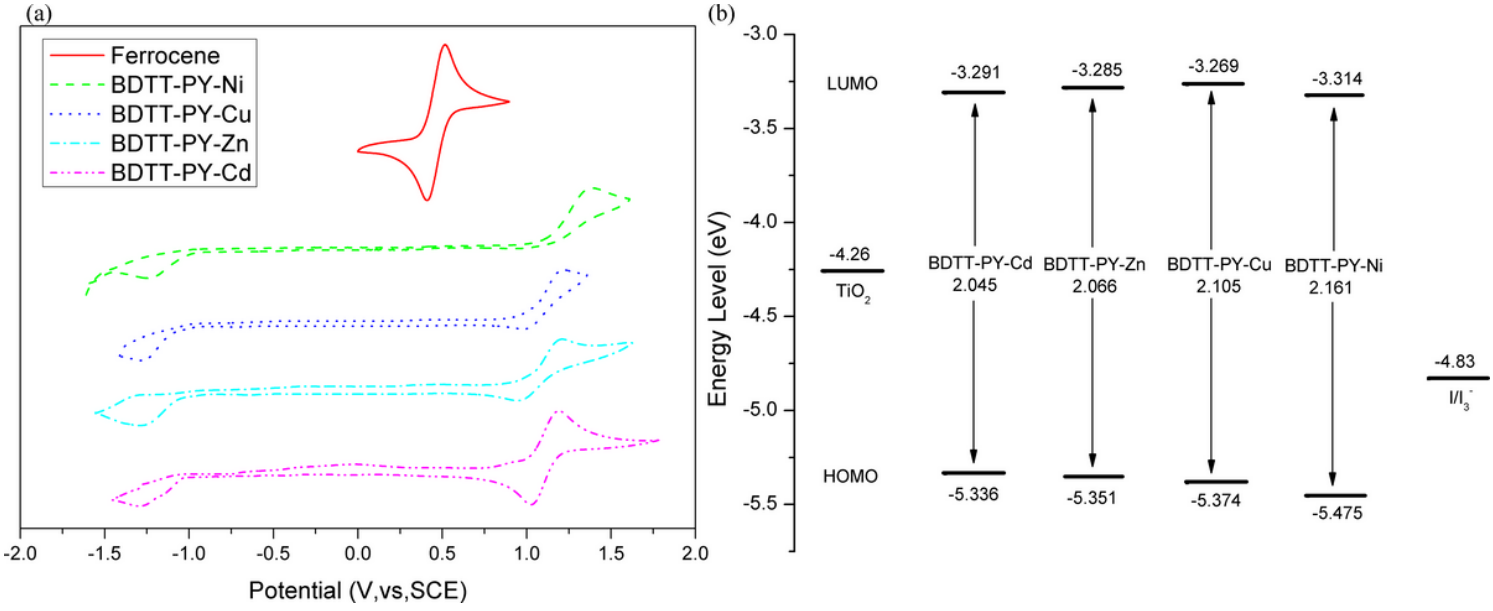

Figure 2

Cyclic voltammetry curves of four polymeric metal complexes BDTT-PY-Cd, BDTT-PY-Zn, BDTT-PY-Cu and BDTT-PY-Ni on glassy carbon electrode in a 0.1 mol L-1 Bu4NBF4 acetonitrile solution at a scan rate of 100 mV s-1 (a) and HOMO and LUMO energy levels of four polymeric metal complexes (b).

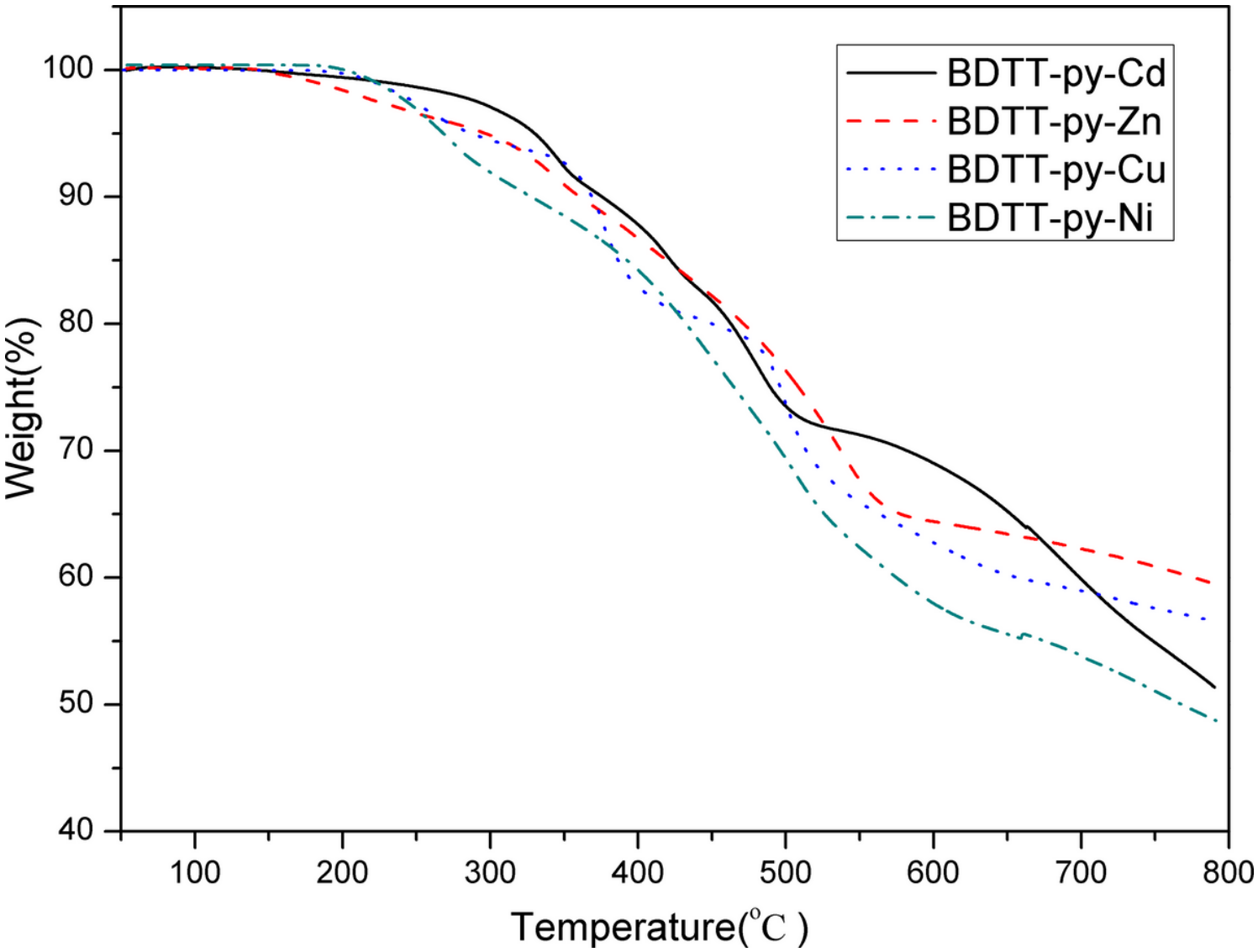

Figure 3

TGA curves of the four polymeric metal complexes with a heating rate of 20°C/min under nitrogen atmosphere.

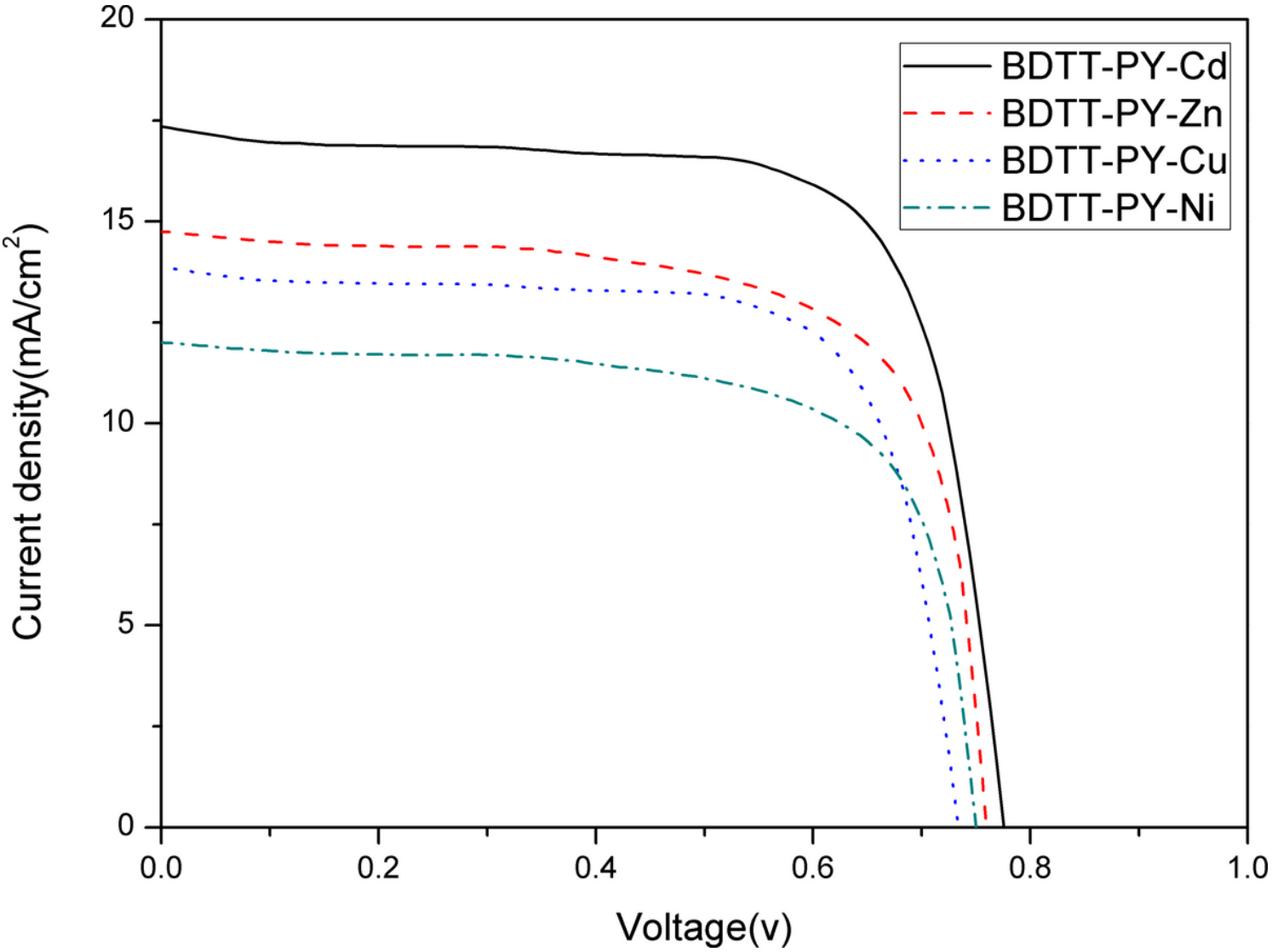

Figure 4

J-V curves and spectra of DSSCs based on four polymeric metal complexes BDTT-PY-Cd, BDTT-PY-Zn, BDTT-PY-Cu and BDTT-PY-Ni under the illumination of AM 1.5, 100 mW cm-2.

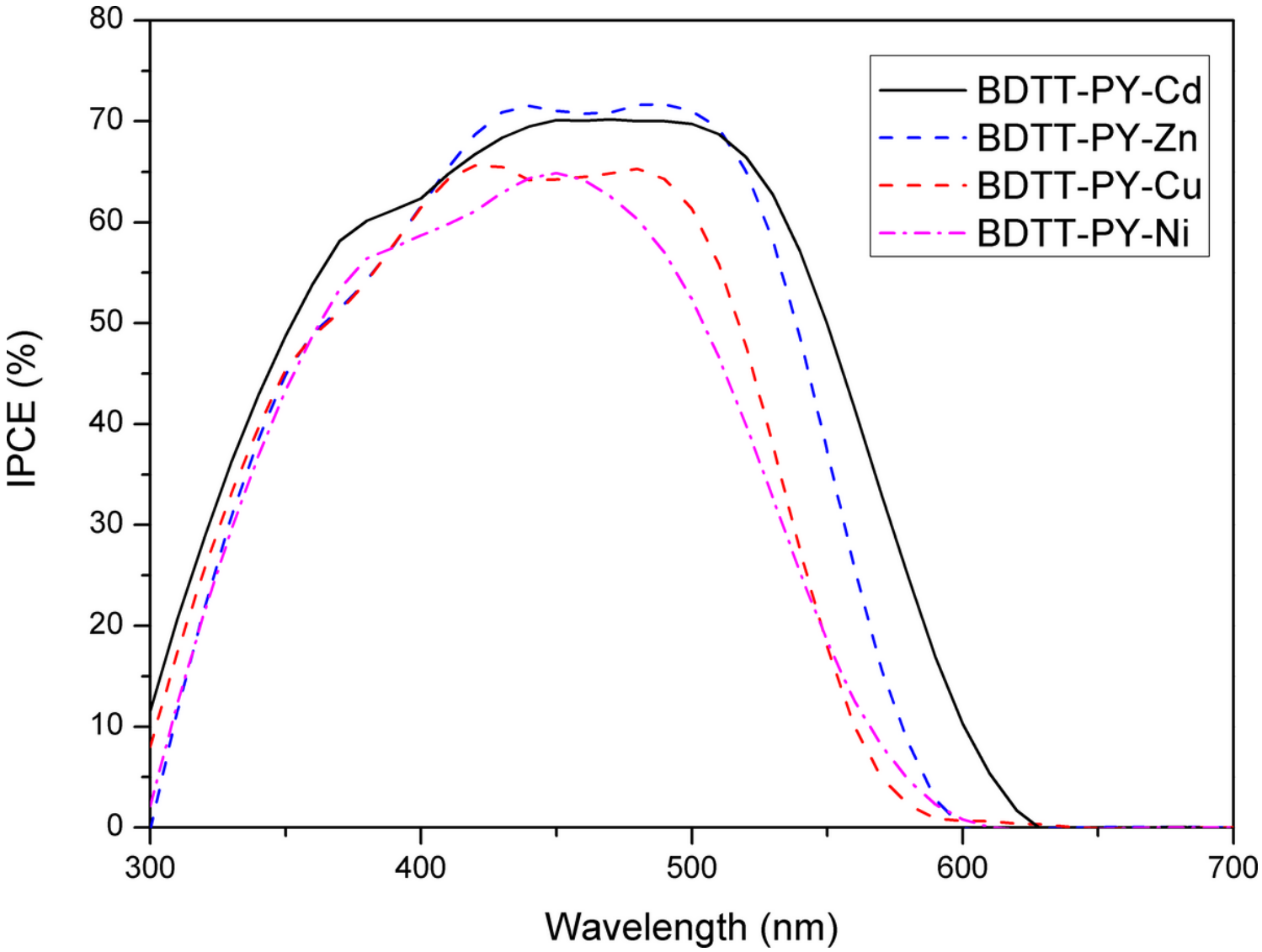

Figure 5

Incident photon-to-current conversion efficiency (IPCE) based on four polymeric metal complexes BDTT-PY-Cd, BDTT-PY-Zn, BDTT-PY-Cu and BDTT-PY-Ni under the illumination of AM 1.5, 100 mW cm-2.

Supplementary Files

This is a list of supplementary files associated with this preprint. Click to download.

- supportinginformation.docx
- scheme1.tif